Characteristic Modified X-Ray Scattering*

K. Das Gupta
W. M. Keck Laboratory of Engineering Materials, California Institute of Technology, Pasadena, California

(Received April 19, 1962)

The spectroscopic analysis of the scattered x rays from lithium, lithium oxide, lithium fluoride, beryllium, and boron irradiated by copper target radiation establishes the existence of sharp characteristic modified lines on the longer wavelength side of the primary beam. This is a new type of incoherent x-ray scattering. The K term values of lithium, beryllium, and boron and the L_1 term value of fluorine in lithium fluoride have been calculated from the observed modified lines and these are 58.1, 113.6, 199.0, and 40.6 eV, respectively. Taking into account the limits of error in these experiments, the term values obtained by this new method agree well with the values obtained by Skinner by the method of soft x-ray spectroscopy. Evidence obtained until now about the angular dependence of intensity of the newly observed modified lines brings up several interesting points helping to understand the particular process of scattering, and these points have been discussed.

INTRODUCTION

WHEN monochromatic x rays are scattered by matter, we have essentially two types of scattering. These are: (a) the Rayleigh scattering, the elastic coherent type, associated with the process in which the electrons of the scattering atom remain in the same energy state before and after the scattering, and (b) the incoherent Compton scattering, associated with the transition of an electron of the scattering atom from an initial state i, to a final state f, in the continuum. The frequency of the scattered ray in the Compton process depends on the scattering angle and the frequency of the primary radiation and is independent of the scattering element. In the continuous transition from the coherent scattering of a bound electron to the Compton scattering of a free electron we should encounter the special case, "the characteristic modified scattering," in which the frequency of the scattered radiation is changed by an amount corresponding to transitions between two bound states of the scattering atom. This is the phenomenon of partial absorption of a photon, the scattering atom being left in a discrete quantum state, and was discovered by Raman in the visible and the ultraviolet region, involving mostly the vibrational and the rotational states of the molecules. The existence of such radiation as a component of scattered x rays has recently been established.[1] DuMond,[2] in a recent article on the Compton effect, reported on the characteristic modified radiation observed by the present author.

In a Compton process the energy equation for the modified scattering is

$$h\nu_0 = h\nu' + h\nu_q + T + \tfrac{1}{2}MV^2, \tag{1}$$

where ν_0 is the frequency of the incident x rays and ν' that of the scattered x rays, $h\nu_q$ is the energy of the photon just sufficient to raise the qth electron of the scattering atom from the qth level to the first unoccupied level above the Fermi surface in the solid material, T is the kinetic energy of the recoil electron, and $\frac{1}{2}MV^2$ is the kinetic energy given to the atom of mass M. The special case of the "characteristic modified scattering" exists when in Eq. (1) the kinetic energy of the recoil electron $T=0$ and $\frac{1}{2}MV^2$ is neglected and the qth electron of the scattering atom is raised from the ground state E_i to the first unoccupied bound state E_f of the scattering atom. We have from Eq. (1) the scattered modified quantum

$$\begin{aligned} h\nu_m &= h\nu_0 - h\nu_q \\ &= h\nu_0 - (E_i - E_f) \\ &= h\nu_0 - \Delta E. \end{aligned} \tag{2}$$

The $\Delta E = (E_i - E_f) = h\nu_q$ is the critical absorption discontinuity for the qth electron of the atom determined by x-ray or ultraviolet absorption spectroscopy.

From Compton's formula for free electrons,

$$\lambda' - \lambda_0 = (h/m_0c)(1-\cos\phi),$$

we have as a first-order approximation

$$\sin(\phi/2) = (h\nu_0 - h\nu')^{1/2}/(2h\nu_0\alpha)^{1/2},$$

where $\alpha = h\nu_0/mc^2$. In the special case when T, the kinetic energy of the recoil electron, is equal to zero, the "characteristic modified quantum" is $h\nu_m$ and the energy balance $(h\nu_0 - h\nu_m)$ is just sufficient to raise the bound electron to the first unoccupied level. Then we have the relation

$$\begin{aligned} \sin(\phi/2) &= (h\nu_0 - h\nu_m)^{1/2}/(2h\nu_0\alpha)^{1/2} \\ &= \Delta E^{1/2}/(2h\nu_0\alpha)^{1/2}. \end{aligned} \tag{3}$$

In Eq. (3), Compton's free-electron formula has been used in the limiting case, when the initial state corresponds to an electron bound to the nucleus and in the final state the electron is just at the periphery of the atom still bound to the nucleus with an extremely small

*Work jointly supported by the U. S. Atomic Energy Commission and the Office of Naval Research.

[1] K. Das Gupta, Nature, **166**, 563 (1950); **167**, 313 (1951); Science & Culture (India), **21**, 542, 624 (1956); Phys. Rev. Letters, **3**, 38 (1959).

[2] J. W. DuMond, *Encyclopedia of Science and Technology* (McGraw-Hill Book Company, Inc., New York, 1960), Vol. 3, p. 353.

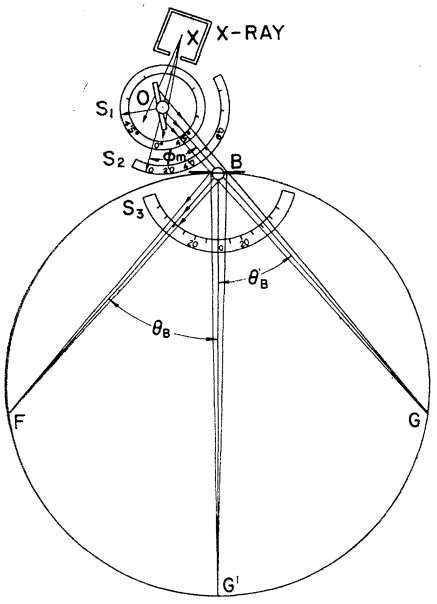

FIG. 1. Schematic sketch of method I. X rays from the "point-focus" copper target X irradiate the scattering material pivoted at 0. The sample orientation with respect to the beam OX could be read against the scale S_1. The scale S_2 fixes the position of the slit tube (not shown) so that the mean scattering angle ϕ_m is known. A second slit tube (not shown) pivoted at B could be adjusted against S_3 such that the rays scattered at ϕ_m makes the proper Bragg angle θ_B to be recorded on a film at F, mounted along the focal circle $FG'G$.

binding energy and the atom is just not ionized. This special type of scattering is hereafter referred to as the "characteristic modified scattering" in which the modified lines are extremely sharp, having the same order of width as that of the primary lines, and they appear at the calculated energy gap from the primary line depending on the binding energy of the involved electron and not on the scattering angle ϕ as in Compton scattering.

The value of the modified quantum $h\nu_m$ is calculated from Eq. (2), knowing the value of ΔE_q for the qth electron of the particular scattering element, and the calculated value could be compared with the experimentally observed value. For scattering angle ϕ less than the critical angle ϕ_q obtained from Eq. (3) for the qth electron, the latter cannot have any contribution to the Compton process, if we ignore the momentum distribution of the bound electron. For values of scattering angles greater than the critical angle ϕ_q, the qth electron will be in the continuous state as the recoil electron contributing to the Compton process. In his investigations of the Compton process with bound electrons, DuMond[3] first clearly established the fact that the energy distribution of the Compton band corresponds to the Doppler broadening produced by the electrons having an initial momentum distribution prescribed for electrons in the atom. The energy width at half-intensity was estimated equal to $4[\Delta E(h\nu_0-h\nu')]^{1/2}$, where ΔE is the binding energy of the electron and $h\nu_0$ and $h\nu'$ are the initial and final photon energies.[4] In a Compton process with bound electrons the energies of the Compton quanta at a particular angle have a certain distribution having the limiting value $h\nu_m=h\nu_0-\Delta E$. With bound electrons the differential Compton cross section at small angles is considerably less compared to that for free electrons, and this could be quite significant for certain relative magnitudes of the incident photon and the binding energy of the electrons involved.

At the scattering angle ϕ_q corresponding to the binding energy ΔE_q the qth electron could be raised to the periphery of the atom, the first unoccupied level, and the characteristic modified quantum $h\nu_m$ would originate, where $h\nu_m=h\nu_0-\Delta E_q$. This is the region of the short-wavelength Compton cutoff where the Compton band due to the tightly bound electrons will be so broad as to be undetectable. It is in this region that the characteristic modified lines originate with maximum intensity and they are also extremely sharp, so the particular scattering process cannot be a typical Compton process. Also to be noted is that the characteristic modified lines appear at the calculated energy gap from the primary line depending on the binding energy of the involved electron and not on the scattering angle ϕ as in Compton effect. The intensity of the characteristic modified lines is, however, dependent on the scattering angle, being maximum at an angle given by Eq. (3). This scattering process cannot be a typical Smekal-Raman process, since the characteristic modified quantum appears with maximum intensity at the scattering angle ϕ given by Eq. (3).

In the formula for the intensity of the Compton scattering as given by Compton, Breit-Dirac, and Klein-Nishina, one point which is highly significant at small angles of scattering has not been considered. A particular lattice plane d_{hkl} of the crystalline-scattering specimen could be oriented normal to the direction of the path of the recoil electron such that the recoil electron experiences a total Bragg reflection. The introduction of this idea would physically mean that the cross section for the Compton process corresponding to the scattering angle ϕ is equal to zero, if the corresponding recoil electron ejected at an angle θ_r to the primary beam $[\cot\theta_r=(1+\alpha)\tan(\phi/2)]$ exactly satisfies the total Bragg reflection condition, λ recoil electron $=h/mv=2d_{hkl}$. It would be interesting to study if the cross section of the characteristic modified scattering process involving the inner-shell electrons would increase when there is such a lattice restriction of the Compton process involving the loosely bound valence-band electrons of the scattering element.

In the present paper the author presents experimental evidence verifying the existence of the char-

[3] J. W. M. DuMond, Revs. Modern Phys. **5**, 1 (1933); J. W. M. DuMond and P. Kirkpatrick, Phys. Rev. **52**, 419 (1937).

[4] J. W. Motz and G. Missoni, Phys. Rev. **124**, 1458 (1961).

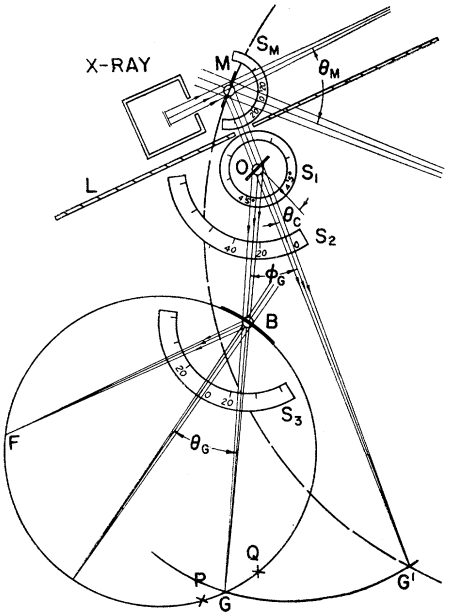

FIG. 2. Two curved crystals for precision scattering work: method II. M is the curved quartz crystal monochromator, plane (110) and radius 10 inches, converging Cu $K\alpha_{1,2}$ to G' passing through the sample pivoted at 0. The scattered beam OBG makes an angle ϕ_G with the primary beam. The bent quartz analyzer spectrograph (310) plane is of $5\frac{1}{2}$ in. radius and could be rotated about B to have the proper Bragg angle θ_G to record the wavelength λ_G at F. A spring adjustment always keeps $OG=OG'$ for different values of ϕ_G. The circular scales S_M, S_1, S_2, and S_3 adjust respectively the positions of the monochromator, the sample with respect to the primary beam, the scattering angle ϕ_G, and the Bragg angle θ_G.

acteristic modified lines in lithium, beryllium, boron, and lithium fluoride, and discusses the angular dependence of intensity based on the experimental results.

EXPERIMENTAL

Method I. Analysis of the Scattered X Rays with a Bent Quartz-Crystal Spectrograph

A schematic sketch of the experimental arrangement is given in Fig. 1. The scattered beam converging to the point G of the focal circle is transmitted through the bent quartz at B and the rays make equal angles θ_B with the bent lattice planes (310) of the quartz crystal. The "point"-focus copper target X of the high-power sealed-off Norelco x-ray tube is within a distance of about 2 in. from the scattering sample pivoted at O. The distances OX and OG could be so adjusted that the spectrograph setting characterizes an ideal defocused condition, so far as the recording of the Compton-scattered radiation is concerned. The Compton band is thus dispersed through a wider area, is weak in intensity, and is not too bad a background for the appearance of the characteristic sharp modified lines. It will be evident from Fig. 1, although the rays constituting the convergent beam OG make equal angles θ_B at the bent lattice planes at B, the scattering angles ϕ of the constituent rays vary continuously about the mean value ϕ_m for a particular setting. Thus, the incoherent part of the scattered beam converging to the point G should consist of rays of smoothly varying wavelengths because in Compton scattering the modified wavelength depends on the scattering angle ϕ. Only that portion of the scattered beam converging to G could be reflected at F for which $\lambda_m=2d_{(310)}\sin\theta_B$ and the rest, having wavelengths other than λ_m, cannot satisfy the Bragg condition of reflection and is completely out of the picture. The mean scattering angle ϕ_m could be selected by adjusting the position of the slit tube with the help of the circular scale S_2, and conveniently enough the deviation $\delta\phi$ could be as large as $\pm 10°$. The effective width of the bent crystal was about 5 mm$\times$2.5 mm and this was helpful in recording quite a region of wavelength, viz., Cu $K\alpha_{1,2}$ and $K\beta_1$ because of the angular range $\delta\theta_B$ at the bent crystal. In fact, the ideal defocused condition for the incoherent Compton scattering turns out to be tremendously useful in recording the characteristic modified scattering, since the Compton background is not too strong to hide the sharp characteristic lines. However, the mean scattering angle ϕ_m could be so adjusted that the Compton band would appear distinctly separated from the characteristic sharp modified lines and this will be discussed in a later section when we treat the angular dependence of intensity of the characteristic modified lines.

Method II. Precision Scattering Work with Two Curved Crystals

To study the angular distribution of intensity of characteristic modified radiation using either single-crystal or polycrystalline material, precision experiments are presently being conducted with two curved crystals—one used as the monochromator and the other as the analyzer spectrograph. When the scattering specimen is polycrystalline, the experimental arrangement as sketched in Fig. 2 is essentially meant for the spectroscopic analysis of the background radiation of the Guinier diffraction pattern which appears along the circle GG'. Such an analysis has been confined to certain specific regions of the background and the reason for such selection will be discussed in a later section. Experiments have also been conducted with a single crystal of LiF in transmission as well as in reflection and the preliminary results indicate both (a) a crystal orientation effect and (b) the dependence of intensity of the characteristic modified lines on the scattering angle ϕ.

The essential merit of the two-curved-crystal arrangement lies in having an ideal focusing condition for the incoherent part of the scattered radiation, within the limits of the rocking-curve widths, without using any slit system. In Fig. 2 the scattered cone of x rays OBG from the sample at O make an angle ϕ_G with the monochromatic primary cone of x rays MOG'. The bent

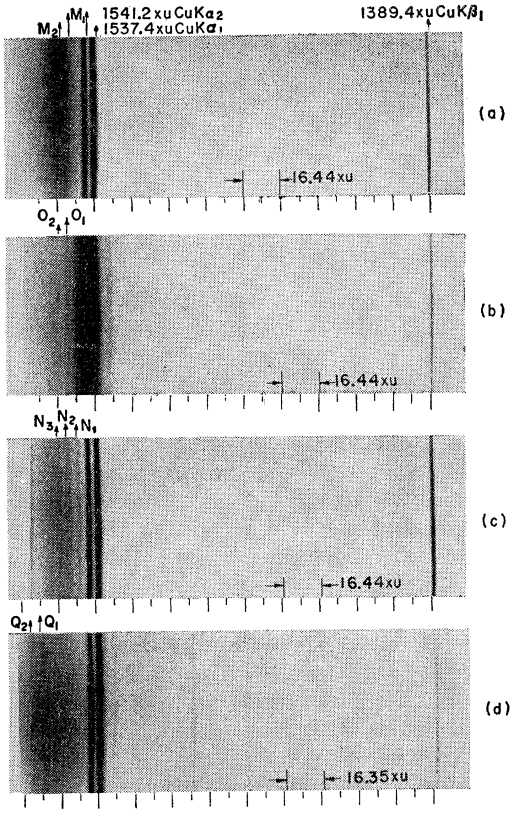

FIG. 3. Enlarged prints of the negative obtained by method I with bent quartz crystal spectrograph 9-in. radius using (310) plane. The Norelco high-power copper-target x-ray tube was run at 40 kV, 30 mA. The characteristic modified lines M_1, M_2, O_1, O_2, etc., all appear on the long-wavelength side of the unmodified primary lines Cu $K\alpha_1$ and $K\alpha_2$. In Fig. 3(b), the Cu $K\alpha_3$ line appears immediately on the short-wavelength side of Cu $K\alpha_1$. (a) Lithium metal: $\phi=55°$, exposure hours: 20; the characteristic modified lines M_1: (Cu $K\alpha_1$—Li K) and M_2: (Cu $K\alpha_2$—Li K) appear superposed over the Compton background. (b) Lithium oxide: $\phi=22°$, exposure hours: 25. O_1: (Cu $K\alpha_1$—Li K) and O_2: (Cu $K\alpha_2$—Li K) are separated from the Compton band which has shifted towards the primary line. (c) Lithium fluoride (Single crystal): $\phi=55°$, exposure hours: 45; N_1: (Cu $K\alpha_1$—F L_1), N_2: (Cu $K\alpha_1$—Li K) and (Cu $K\alpha_2$—F L_1) superposed; N_3: (Cu $K\alpha_2$—Li K), the Compton background is fairly weak in intensity. (d) Beryllium metal: $\phi=81°$, exposure hours: 45; Q_1: (Cu $K\alpha_1$—Be K) and Q_2: (Cu $K\alpha_2$—Be K) the peak of the Compton band is immediately on the short-wavelength side.

crystal of the analyzer spectrograph pivoted at B could be adjusted to a position so as to receive the scattered cone of x rays OBG at Bragg angle θ_G such that $\lambda_G=2d_{(310)}\sin\theta_G$ and the value of λ_G, the modified Compton wavelength, is determined accurately by the scattering angle ϕ_G. Any other cone of x rays from the sample at O converging to the point Q on the right side of G would be scattered at an angle $\phi_Q<\phi_G$. But the cone of x rays OBQ would make, at the bent-quartz lattice planes at B, an angle $\theta_Q>\theta_G$. According to Compton's formula, the modified wavelength λ_G must be greater than the modified λ_Q, since $\phi_G>\phi_Q$. But the experimental arrangement is such that $\theta_G<\theta_Q$. From Fig. 2 it will be at once evident that, if the analyzer spectrograph is adjusted to reflect λ_G at Bragg angle θ_G, then for the same position of the spectrograph λ_Q cannot have any Bragg reflection because λ_Q makes an angle θ_Q with the bent crystal which is greater than θ_G but, by Compton's relation, $\lambda_Q<\lambda_G$. A similar argument will show that the cone of scattered x rays OPB cannot be reflected for the same θ_G setting of the spectrograph because for any point P on the left-hand side of G, $\lambda_P>\lambda_G$ but $\theta_P<\theta_G$.

Thus, the Bragg formula and the Compton formula cooperate so as to focus for a fixed setting of the analyzer spectrograph only a particular value of the modified wavelength, and this becomes an ideal arrangement to get rid of the Compton background, enabling us to record only the characteristic sharp modified lines.

Adopting the experimental method II,[5] using the single crystal of LiF as the scattering specimen, preliminary experiments have been done at scattering angle $\phi=55°$. With an exposure of 50 h the modified lines appear at the calculated position but are extremely weak in intensity. Improvements in the accurate adjustments are being made, using more precise circular scales (S_1, S_2, and S_3 in Fig. 2).

RESULTS

Experiments were done with metallic lithium, lithium fluoride (as pressed powder, as well as in single-crystal form), lithium oxide, beryllium, and boron as the scattering materials, adopting the experimental method I as shown in Fig. 1. Successful photographs have been obtained showing sharp characteristic modified lines

TABLE I. Copper K lines,[a] absorption edges of the scattering elements,[b] calculated and experimental values of characteristic modified lines. The dispersion on the original negative is 8 xu/mm and the limit of error is ±2 xu or ±10 eV (transformation factor 12 372.2×10³ eV xu⁻¹).

Emission lines	xu	eV	Absorption edges	xu	eV
Copper $K\alpha_1$	1537.4	8047.4	Lithium K	226.1	54.7
Copper $K\alpha_2$	1541.2	8027.6	Beryllium K	110.6	111.8
Copper $K\beta_1$	1389.4	8905.0	Boron K	66.0	186.4
			[c]Fluorine L_1	381.8	32.4

Scattering specimen	Modified line scheme	Wavelength xu Calc.	xu Expt.	Energy eV Calc.	eV Expt.
Lithium metal	Cu $K\alpha_1$—Li K	1548.0	1548.6	7992.4	7989.3
	Cu $K\alpha_2$—Li K	1551.7	1553.0	7973.0	7966.6
Lithium in LiF single crystal	Cu $K\alpha_1$—Li K	1548.0[d]	1549.2	7992.4	7986.2
	Cu $K\alpha_2$—Li K	1551.7[d]	1554.0	7973.0	7961.6
Lithium in Li_2O (powder)	Cu $K\alpha_1$—Li K	1548.0[d]	1549.4	7992.4	7985.1
	Cu $K\alpha_2$—Li K	1551.7[d]	1553.4	7973.0	7964.5
Beryllium metal	Cu $K\alpha_1$—Be K	1559.1	1561.4	7935.4	7923.8
	Cu $K\alpha_2$—Be K	1563.0	1565.4	7915.6	7903.6
Boron metal (fine powder)	Cu $K\alpha_1$—B K	1573.8	1576.4	7861.0	7848.4
	Cu $K\alpha_2$—B K	1577.8	weak	7841.2	weak
Fluorine in LiF single crystal	Cu $K\alpha_1$—F L_1	1543.6	1545.2	8015.0	8006.8
	Cu $K\alpha_2$—F L_1	1547.5	1549.2	7995.2	7986.2

[a] A. E. Sandstrom, in *Handbuch der Physik*, edited by S. Flügge (Springer-Verlag, Berlin, 1957), Vol. 30, p. 182.
[b] H. W. B. Skinner, Phil. Trans. Roy. Soc. London **A239**, 95 (1940).
[c] Value estimated by extrapolation.
[d] The absorption edges of lithium in LiF and Li_2O being unknown, the calculated value is for metallic lithium.

[5] The experimental technique has been described in detail in an unpublished Technical Report No. 5 to the sponsoring agencies (May, 1962). Requests for the report should be sent to the author.

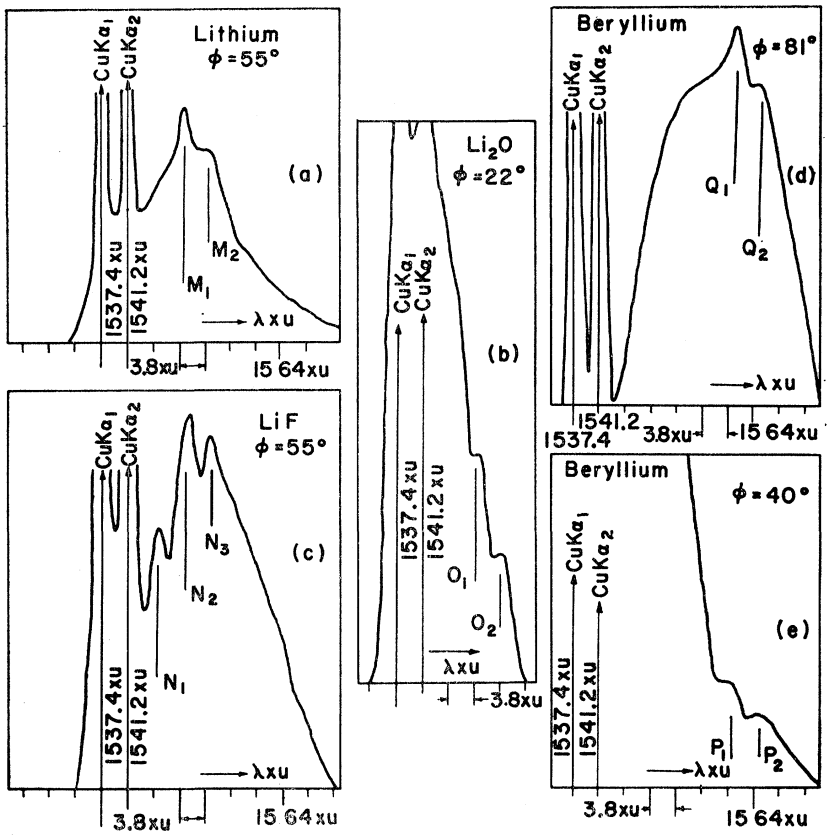

FIG. 4. Microphotometer records (10 times magnified) showing the Rayleigh, the Compton, and the characteristic modified scattering of x rays. (a), (b), (c), and (d) are the photometer records of the negatives for which the enlarged prints have been shown in Figs. 3(a), (b), (c), and (d) in respective orders. (e) is the photometer record for beryllium at $\phi=40°$; the characteristic modified lines, P_1: (Cu $K\alpha_1$—Be K) and P_2: (Cu $K\alpha_2$—Be K), appear completely separated from the Compton band which shifts towards the unmodified lines.

at calculated energy gaps on the longer wavelength side of the primary beam. The observed and the calculated values of the characteristic modified lines are given in Table I, the measurements being made on the original negatives with the Norelco film-measuring device. The enlarged prints of the negatives are shown in Figs. 3(a)' (b), (c), and (d) and their photometer records in respective orders are given in Figs. 4(a), (b), (c), and (d). The essential features of the experimental results may be summarized as follows:

1. The wavelengths of the characteristic modified lines are independent of the scattering angle and depend only on the incident photon energy and the term value of the bound electron of the scatterer.

2. The characteristic modified lines are sharp, having the same order of width as that of the primary incident radiation.

3. The intensity of the characteristic modified lines is maximum at scattering angles given by Eq. (3), when they appear more or less superimposed on the usual Compton band.

4. At smaller values of scattering angles, the usual Compton band shifts towards the primary line but the characteristic modified lines do not shift in position and appear distinct on a clearer background.

5. Within the experimental error the calculated values of the characteristic modified lines agree well with the experimental values.

Lithium Metal and Lithium Oxide

A piece of metallic lithium, 1 cm×1 cm and 3 mm in thickness, coated on all sides with a thin layer of Duco cement, was mounted vertically at O, Fig. 1, and tilted 27°30′ respect to the central ray OX and the scattered x rays at $\phi=55°$ passes through the bent crystal at B. The Bragg angle at B is θ_B so as to reflect at F the characteristic modified lines (Cu $K\alpha_{1,2}$—Li K). To calculate the wavelength of the particular characteristic modified line, the difference in energy between copper $K\alpha_1$ and lithium K edge is converted into wavelength. The K term values of lithium, beryllium, and boron are known directly from the soft x-ray spectroscopic data. The enlarged print, Fig. 3(a), and the photometer record, Fig. 4(a), show the characteristic modified lines superimposed on the Compton band. The same sample contaminated with an oxide layer was used to study the scattered radiation at $\phi=22°$. The Compton band shifts towards the unmodified primary lines, and the characteristic modified lines are now separated from the Compton band and appear on a clear background on the longer wavelength side of the usual Compton band, Fig. 3(b) and Fig. 4(b). Table I shows the agreement between the observed and the calculated values of the characteristic modified lines.

Lithium Fluoride

Both single crystals and pressed powder of LiF were used. According to Eq. (3) the maximum intensity of the characteristic modified line (Cu $K\alpha_{1,2}$—F L_1) should appear at 39° and (Cu $K\alpha_{1,2}$—Li K) at 55°. With pressed powder of LiF at $\phi=39°$ the characteristic modified lines due to fluorine L_1 were obtained with an exposure of 15 h at 40 kV, 30 mA using the (310) plane of quartz spectrograph, and with an exposure of 12 h at the same rating using the (100) plane of the quartz spectrograph. With pressed powder of LiF at $\phi=22°$ with an exposure of 45 h at 40 kV, 30 mA, the characteristic modified lines appear without the Compton background, and using the (310) plane of the quartz the lines were nicely resolved, allowing an accurate measurement. Using a single crystal[6] of LiF in transmission, as well as in reflection, with the (200) plane parallel to the vertical axis, the spectroscopic analysis of the scattered radiation was done at $\phi=22°$, 39°, 42°, and 55° using the (310) plane of the bent-quartz spectrograph, intensity being sacrificed for the sake of higher resolution. The characteristic modified lines due to fluorine L_1 did appear in all the experiments, but that due to lithium K appeared strongly only at $\phi=55°$. At scattering angles less than 55° there is only a faint indication of the characteristic modified line due to Li K. Figure 3(c) and Fig. 4(c) show the enlarged print and the photometer record of the original negative recording the scattered radiation from the single crystal of LiF (in reflection) at $\phi=55°$, the characteristic modified line (Cu $K\alpha_2$—F L_1) appears almost in the same position as the line (Cu $K\alpha_1$—Li K). The widths of the characteristic modified lines agree with the width of the primary line.

Beryllium

A piece of polycrystalline beryllium, about 4 sq mm in area, has been used in reflection at $\phi=81°$ and at $\phi=40°$. With an exposure of 45 h at 40 kV and 30 mA, at $\phi=81°$, an excellent picture was obtained, Fig. 3(d) and Fig. 4(d). The characteristic modified lines (Cu $K\alpha_{1,2}$—Be K) appear quite strong, although superimposed on to the Compton background. The peak of the usual Compton band is immediately on the short-wavelength side of the characteristic modified lines. With the photograph at $\phi=40°$ the characteristic modified lines appear distinctly separated from the Compton background as shown in Fig. 4(e), the Compton peak shifting towards the primary line. The width of the characteristic modified line measured on the original negative agree with the width of the primary lines.

Boron

With extremely fine powder of boron the scattering experiment was done at $\phi=127°$ which, according to Eq. (3), should be the scattering angle to get the maximum intensity for the characteristic modified line. The line appeared weak with an exposure of 25 h at 40 kV and 30 mA. Measurements made on the original negative show excellent agreement between the observed and the calculated line within allowed experimental error.

[6] Supplied by Harshaw Chemical Company.

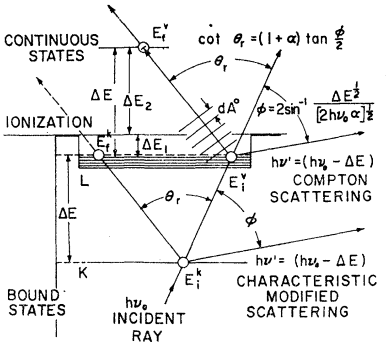

FIG. 5. Schematic energy level diagram indicating the Compton and the characteristic modified scattering processes at the short-wavelength Compton cutoff limit, when $\phi=2\sin^{-1}[\Delta E^{1/2}/(2h\nu_0\alpha)^{1/2}]$. The mechanism of the lattice restriction of the recoil electrons from the valence band has been shown.

INTERPRETATION

A schematic energy-level diagram indicating the scattering process has been drawn in Fig. 5. This is divided into two sections, the bound states at the bottom and the continuous states at the top of the ionization level. When the incident primary beam $h\nu_0$ knocks out any of the electrons in bound states, we calculate the kinetic energy $T=h\nu_0-\Delta E_q$, where ΔE_q is the binding energy of the qth electron. This is the photoelectric effect, and the electron is in the continuous state.

In the Compton process a partial absorption of the photon is possible, raising the bound electron to the continuous state depending on the amount of the energy transfer from the incident photon which is related to the direction of the scattered Compton quantum. In a Compton collision with bound electrons, the energy of the photons scattered at a particular angle is not uniquely determined and this is distributed from zero to $(h\nu_0-\Delta E)$, where $h\nu_0$ is the incident photon energy and ΔE is the binding energy of the electron. It will be interesting to calculate the mode of distribution in the case of K-shell electrons of lithium, beryllium, and boron with incident copper $K\alpha$ radiation for different scattering angles.

Let us take a specific case when, in Fig. 5, the incident $h\nu_0=8047$ eV for copper $K\alpha_1$ and the scattering element is lithium metal. The valence band width of lithium metal is about 4 eV and the K absorption edge corresponds to the transfer of a K ($1S$) electron to the first unoccupied level immediately on the top of the Fermi surface, and this will be a $2p$ state to allow the transi-

TABLE II. Critical values of the scattering angles ϕ_q in column (2) are shown against the energy gap ΔE, column (1), for primary Cu $K\alpha_1$ radiation, using Eq. (3). Columns (3) and (4) show the d and 2θ values of the strong reflection planes for Cu $K\alpha_1$. Column (5) shows the scattering angles at which the corresponding recoil electrons would experience total Bragg reflection, restricting the Compton process of the valence band electrons.

Specimen	ΔE (eV) (1)	$\phi_q=2\sin^{-1}[\Delta E^{\frac{1}{2}}/(2h\nu_0\alpha)^{\frac{1}{2}}]$ $=2\sin^{-1}(0.0627\times\Delta E^{\frac{1}{2}})$ (2)	d (Å)[a] (3)	2θ (4)	$\phi_n=2\tan^{-1}(0.385/d)$ (5)
Lithium K	54.7	55°	2.48 (100)[a]	36°12′	17°18′
			1.75 (17)	52°12′	24°30′
			1.43 (20)	65°12′	29°46′
Beryllium K	111.8	81°	1.97 (20)	46°	21°50′
			1.79 (14)	51°	24°16′
			1.73 (100)	53°	24°46′
Lithium fluoride	Li $(K)=54.7$	55°	2.325 (95)	38°48′	18°34′
	F $(L_1)=32.4$	39°	2.013 (100)	45°	21°24′
	LiF $(V)>9$	>21°24′	1.424 (48)	65°30′	29°52′

[a] Values of I/I_1 in percent are given in parentheses.

tion. In metals, the K absorption edge corresponds to the short-wavelength K emission edge, which is 54.7 eV in lithium. With respect to the incident beam of 8047-eV energy let us assume that both K-shell and valency electrons of lithium contribute to the Compton process, obeying more or less Compton's free-electron formula. As shown in Table II, column (2), the most probable energy transfer to the recoil electrons corresponding to the degradation of the incident photon $h\nu_0$ at the scattering angle $\phi=55°$ is 54.7 eV by Eq. (3). For $\phi=55°$, the K-shell electron of lithium will be transferred to the first unoccupied level on the top of the Fermi surface, $E_i^K-E_f^K=\Delta E=54.7$ eV, which corresponds to the short-wavelength Compton cutoff involving K-shell electrons of lithium. The characteristic modified quantum would originate, having maximum intensity at $\phi=55°$ corresponding to the short-wavelength Compton cutoff. For ϕ less than 55° it will be evident that K-shell electrons cannot contribute to an ideal Compton process. However, due to another channel of interaction, the valence band electrons of lithium must appear in the continuous states contributing to the usual Compton process at $\phi=55°$, reflecting the momentum distribution of the valence-band electrons as shown by DuMond.

Using Compton's free-electron formula, the kinetic energy of the recoil electrons originating from the metal valence band can be calculated for the scattering angle ϕ and the direction of the recoil electron θ_r ascertained. From the expression for the kinetic enegry of the recoil electron its momentum could be ascertained and, hence, the de Broglie wavelength $\lambda=h/mv$ for the recoil electrons ejected at an angle θ_r will be known. Using $\lambda=2d$ for the total Bragg reflection condition of the recoil electron within the crystal, one gets the approximate relation

$$d_{hkl}\cos\theta_r=d_{hkl}\tan(\phi/2)=0.385 \qquad (4)$$

in the case of copper $K\alpha_1$ radiation. In formula (4), d_{hkl} is the particular lattice spacing of the scattering specimen which is oriented so as to receive normally the recoil electron ejected at an angle θ_r to the primary beam as shown in Fig. 5. The d values of the strong reflection planes and 2θ values for copper $K\alpha_1$ ($\theta=$Bragg angle) are given in Table II, columns (3) and (4). The scattering angles ϕ corresponding to which the recoil electrons cannot originate would simply physically mean that the Compton cross section will be zero for those values of ϕ, given by the formula (4). Table II, column (5), shows that for the strong reflection planes of lithium, beryllium, and lithium-fluoride the scattering angle ϕ for which there cannot be any Compton collision lies within 17°18′ to 29°52′. Scattering experiments conducted at values of ϕ within this range would show a considerable decrease in the differential Compton cross section for most of the crystalline materials because of the fact that most crystals have strong reflection planes more or less at small Bragg angles as shown in column (3) of Table II. Corresponding to $\phi=17°$ and $\phi=30°$ the ΔE values, as given by the Eq. (3), are approximately 5.5 and 15 eV, respectively. It is expected that for the scattering specimens for which the ΔE values in column (1) are such that the angles ϕ_q in column (2) are of the same order of magnitude as the angles ϕ_n in column (5) of the Table II, the characteristic modified lines would appear strongest.

If we consider the strongly diffracted beams at definite angles within the scattering specimen due to Bragg reflection, it is obvious that for the scattering angle ϕ the other effective values for ϕ will be $(\phi\pm 2\theta_{hkl})$, where θ_{hkl} is the Bragg angle for the plane hkl. Experiments are in progress to ascertain the angular dependence of intensity of the characteristic modified lines considering these effects of multiple scattering.

It is well known that the differential Compton cross section at small angles is less for a bound electron than for a free electron. Also, the more tightly bound electrons give rise to so broad a Compton band as to be undetectable. Again at small angles of scattering, there

is always a possibility of the lattice restriction of the Compton process due to the total Bragg reflection condition of the recoil electrons according to formula (4). Considering the above facts, it is reasonable to argue that the characteristic modified lines would be best expected at small angles of scattering because the other normal channels of Compton interaction with both free and bound electrons are highly restricted at small angles of scattering.

ACKNOWLEDGMENTS

The author is grateful to Professor Pol Duwez for providing him with the research facilities in his laboratory and for his great interest in the particular problem and his helpfulness. Thanks are due to Dr. F. S. Buffington for going through the manuscript. The author is grateful to Professor J. W. M. DuMond for his encouragement and to Professor R. P. Feynman for valuable discussions.

PHYSICAL REVIEW VOLUME 128, NUMBER 5 DECEMBER 1, 1962

Multiple Scattering of Neutrons in the Static Approximation

J. H. FERZIGER AND A. LEONARD*
Nuclear Engineering Laboratory, Stanford University, Stanford, California
(Received June 20, 1962; revised manuscript received August 27, 1962)

It is shown that, within the static approximation, the neutron diffraction pattern from a sample can be interpreted in terms of multiple particle correlation functions. In particular, the relation between double scattering and the three-particle correlation function is derived. Although the formula given cannot be formally inverted to give the three-particle correlation function, it may be useful for making corrections for multiple scattering in experiments.

INTRODUCTION

MUCH work has been done in the areas of elastic scattering of neutrons and x-ray diffraction from both solids and liquids, dating to the early work of Zernike and Prins.[1] It is readily demonstrated by means of the first Born approximation that the diffraction pattern can be interpreted in terms of the two-particle time-independent correlation function. More recently, Van Hove[2] and others have shown how inelastic neutron scattering may be described in terms of a time-dependent two-particle correlation function.

It is well known that this relation between the two-particle correlation function and the single-scattering diffraction pattern arises from the interference of the waves scattered from different nuclei. If, however, a neutron makes more than one collision in a sample, the diffraction pattern should be sensitive to the positions of more than two nuclei. For example, the pattern arising from the interference between singly scattered neutrons and twice scattered neutrons can be expected to be related to the three- and four-particle distribution functions.

In this paper the above statement is proven and it is shown how higher order correlation functions are related to higher order multiple scattering. Unfortunately, the results derived do not enable one to calculate the three-particle correlation function from the results of a diffraction experiment. The converse, however, is true and the results may be useful for estimating the contribution of multiple scattering to the observed diffraction patterns. Thus, a simple correction for multiple scattering effects can be made.

THE SECOND BORN APPROXIMATION

Using a semiclassical approach and assuming that the nuclei of the scatterer are alike and stationary, the second Born (double scattering) approximation to the scattering cross section can be written

$$\sigma(\theta)=\left|\sum_n a_n e^{i\mathbf{K}\cdot\mathbf{r}_n}+\sum_{n,m}{}' a_n a_m e^{i\mathbf{k}\cdot\mathbf{r}_m}e^{-i\mathbf{k}'\cdot\mathbf{r}_n}\frac{e^{ik|\mathbf{r}_n-\mathbf{r}_m|}}{|\mathbf{r}_n-\mathbf{r}_m|}\right|^2, \tag{1}$$

where $\mathbf{k}$=incoming wave vector, $\mathbf{k}'$=outgoing wave vector, $\mathbf{K}=\mathbf{k}-\mathbf{k}'$=scattered wave vector (momentum transfer vector), $\mathbf{r}_n$=position vector of the n^{th} nucleus, and the prime on the summation means that the $m=n$ terms are to be omitted from the sum. The square of the first term in the brackets in Eq. (1) is known to be related to the two-particle correlation function.

Restricting our attention now to the cross-product term, we have

$$\sum_l a_l e^{-i(\mathbf{k}-\mathbf{k}')\cdot\mathbf{r}_l}\sum_{m,n}{}' a_m a_n e^{i\mathbf{k}\cdot\mathbf{r}_m}e^{-i\mathbf{k}'\cdot\mathbf{r}_n}\frac{e^{ik|\mathbf{r}_n-\mathbf{r}_m|}}{|\mathbf{r}_n-\mathbf{r}_m|}+\text{C.C.} \tag{2}$$

Assuming the scattering lengths to be uncorrelated (i.e., random spin and isotope disorder) the first term of

* Atomic Energy Commission Fellow.
[1] F. Zernike and J. Prins, Z. Physik **41**, 184 (1927).
[2] L. Van Hove, Phys. Rev. **95**, 249 (1954).

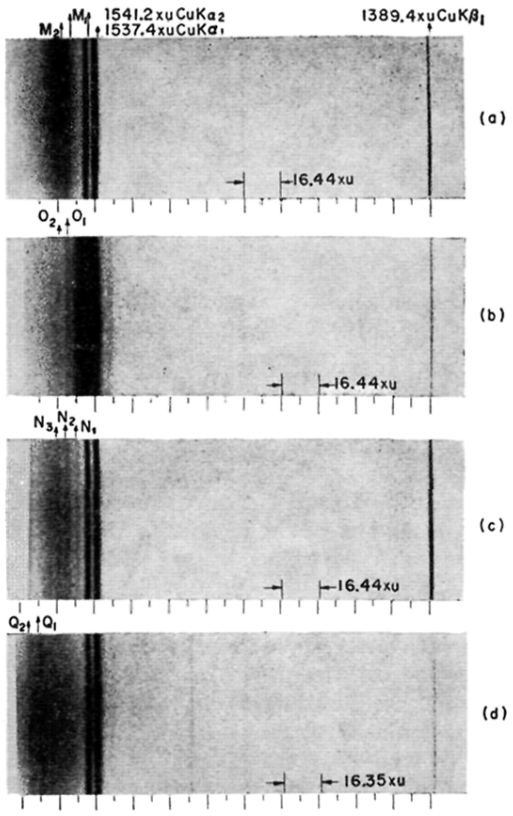

FIG. 3. Enlarged prints of the negative obtained by method I with bent quartz crystal spectrograph 9-in. radius using (310) plane. The Norelco high-power copper-target x-ray tube was run at 40 kV, 30 mA. The characteristic modified lines M_1, M_2, O_1, O_2, etc., all appear on the long-wavelength side of the unmodified primary lines Cu $K\alpha_1$ and $K\alpha_2$. In Fig. 3(b), the Cu $K\alpha_3$ line appears immediately on the short-wavelength side of Cu $K\alpha_1$. (a) Lithium metal: $\phi=55°$, exposure hours: 20; the characteristic modified lines M_1: (Cu $K\alpha_1$−Li K) and M_2: (Cu $K\alpha_2$−Li K) appear superposed over the Compton background. (b) Lithium oxide: $\phi=22°$, exposure hours: 25. O_1: (Cu $K\alpha_1$−Li K) and O_2: (Cu $K\alpha_2$−Li K) are separated from the Compton band which has shifted towards the primary line. (c) Lithium fluoride (Single crystal): $\phi=55°$, exposure hours: 45; N_1: (Cu $K\alpha_1$−F L_1), N_2: (Cu $K\alpha_1$−Li K) and (Cu $K\alpha_2$−F L_1) superposed; N_3: (Cu $K\alpha_2$−Li K), the Compton background is fairly weak in intensity. (d) Beryllium metal: $\phi=81°$, exposure hours: 45; Q_1: (Cu $K\alpha_1$−Be K) and Q_2: (Cu $K\alpha_2$−Be K) the peak of the Compton band is immediately on the short-wavelength side.